Development of an equivalent composite honeycomb model : a finite element study

Development of an equivalent composite honeycomb model: a finite element study

G. Steenackers[a,b1], J. Peeters[a], B. Ribbens[a] and C. Vuye[c]
[a] *University of Antwerp, Op3Mech research group, Salesianenlaan 30, B-2660 Antwerp, Belgium*;
[b] *Vrije Universiteit Brussel (VUB), Department of Mechanical Engineering (MECH), Acoustics & Vibration Research Group (AVRG), Pleinlaan 2, B-1050, Brussels, Belgium*;
[c] *University of Antwerp, EMIB research group, Paardenmarkt 92, B-2000 Antwerp, Belgium*
University of Antwerp, Faculty of Applied Engineering, Salesianenlaan 90, 2660 Hoboken

Abstract

Finite element analysis of complex geometries such as honeycomb composites, brings forth several difficulties. These problems are expressed primarily as high calculation times but also memory issues when solving these models. In order to bypass these issues, the main goal of this research paper is to define an appropriate equivalent model in order to minimize the complexity of the finite element model and thus minimize computation times. A finite element study is conducted on the design and analysis of equivalent layered models, substituting the honeycomb core in sandwich structures. A comparison is made between available equivalent models. An equivalent model with the right set of material property values is defined and benchmarked, consisting of one continuous layer with orthotropic elastic properties based on different available approximate formulas. This way the complex geometry does not need to be created while the model yields sufficiently accurate results.

Keywords:
Composite structures, Finite Element analysis, numerical modeling, lightweight structures

1. Introduction

1.1. Mechanical Properties of Honeycomb Sandwich Panels

Innovation technologies in aircraft design, automotive applications and lightweight constructions formed the basis for the development of lightweight sandwich panels consisting of a honeycomb structured layer [1]. Honeycomb structures are often used in composite sandwich panels. Due to their impact-resistant properties, honeycomb panels are becoming increasingly popular as shock-absorbing materials combining minimal weight and high bending stiffness [2].

Mainly due to their geometric complexity, it is time consuming and computationally demanding to create a detailed finite element (FE) model in order to analyze their mechanical behaviour. In this paper, the goal is to examine the different approximative formulas based on literature study and to validate the feasibility of a possible substitute model which can replace the highly detailed honeycomb structure in a finite element model. This way the FE calculation time can be seriously reduced.

A highly detailed honeycomb geometry is used as a benchmark model. In the next step, the equivalent models are generated where the honeycomb sandwich layer will be replaced by a solid material layer with orthotropic material properties. These equivalent models will be compared with the highly detailed FE reference model with respect to accuracy and calculation times. The equivalent model that scores best on both parameters can then be used as surrogate orthotropic material layer to replace the honeycomb layer.

Finite element modelling is often applied in honeycomb material analysis and research [3, 4, 5, 6, 7], especially when examining the dynamic behaviour of the composite structure. The idea of carrying out FE simulations on honeycomb panels in order to identify the material specifications dates back from the 1980s. Chamis et al. [8], Karlsson en Wetteskog [9], Martinez [10] en Elspass [11, 12] were using NASTRAN models to identify the nine independent elastic property values. Comparable studies are performed by Mistou et al. [13] on aluminum honeycomb, by Foo et al. [14] on Nomex honeycomb and by Allegri et al. [15] on carbon fibre reinforced honeycomb materials.

The aforementioned studies are always based on ideal, uniform, hexagonal honeycomb cells without imperfections, which in reality is often not the case [16]. The way that cell anomalies are manifesting themselves in the honeycomb structure and respective deviated analysis results, is discused by Hohe en Becker [17]. The influence of irregular cell thickness and geometry on the mechanical properties is analyzed by Li et al. [18], Yang et al. [19] (cell thickness variation), Simone and Gibson [20, 21] (thickness variations of cell boundaries, cell curvature and cross section) and finally Guo and Gibson [4] (elimination of cells). In all these papers, a finite element model of the honeycomb core layer was used.

1.2. Orthotropic Equivalent Model

The equivalent models are generated by replacing the complex honeycomb geometry by a solid material layer with orthotropic properties. In scientific literature, there is a number of studies that try to derive the values of these orthotropic constants. A complete set of 9 elastic constants for honeycomb layers is difficult to trace in literature as the reference papers mainly focus on a partial subset of these constants. Masters en Evans [22] designed a theoretical model to determine E_1, E_2, ν_{12} and G_{12} in two dimensions with the focus on bending and strain mechanisms. They combined the results into a general model that is able to reproduce different results.

Qunli Liu [23] developed equivalent formulae for E_3, G_{13} and G_{23}. Abd-el Sayed, Jones and Burgess [24] focused on E_1, E_2 and ν_{12} in two dimensions. Grediac [25] and Shi & Tong [26] independently calculated G_{13} and G_{23}. Both references started from the studies performed by Kelsey et al. [27]. Grediac used one quarter of a honeycomb cell as a reference cell and applied symmetry rules to simplify the finite element calculations. As a result, the shear modulus is calculated. Becker [28] formulated $E_1, E_2, \nu_{12}, \nu_{32}$ and G_{12} by taking into account the thickness of the honeycomb core. Zhang & Ashby [29] retrieved formulas for $E_3, \nu_{32}, \nu_{13}, G_{13}$ and G_{23} in the case of loading perpendicular to the material layer surface. Buckling, delamination and fracture are identified as probability to failure. E. Nast [30] performed a honeycomb layer study that is comparable to the work of Abd-el Sayed, Jones en Burgess. Nast applied different boundary conditions and achieved formulas for the complete set of nine elastic constants. In Section 2 an overview is given of the approximative formulae which will be used further in Section 5 for reduction of computation times.

2. Formulae for Orthotropic Elastic Constants

In this section different approximations for the determination of the elastic constants are listed. The complete list can be found in appendix. The definition of the used symbols are found in the nomenclature list (Section 7). There are mathematical relationships between the different formulae that yield acceptable approximations. These relationships will be expressed by a K-factor in order to simplify the use of the different approximations with varying geometric parameters. The K-factor will be defined as the ratio of E_3 approximated by Liu [23] and E_2 approximated by Masters & Evans [22].

Calculation of E_3

The following formula for the calculation of E_3 is generally accepted and can be found in the publications of Nast, Liu & Zhang [30, 23, 29]:

$$E_3 = \frac{2.E.t_c}{\cos\varphi.(1+\sin\varphi).a} \tag{1}$$

Calculation of E_2

The following formula for the calculation of E_2 is developed by Masters & Evans [22]:

$$E_2 = \frac{E}{\frac{1+\sin\varphi}{\cos\varphi}.\left[\frac{\sin^2\varphi.a^3}{t_c^3} + \frac{(cos^2\varphi).t_c}{a}\right]} \tag{2}$$

Dividing Eq. (1) by Eq. (2), yields for K-factor:

$$K = \frac{E_3}{E_2} = \frac{\left(\frac{2.E.t_c}{\cos\varphi.(1+\sin\varphi).a}\right)}{\left(\frac{E}{\frac{1+\sin\varphi}{\cos\varphi}.\left[\frac{\sin^2\varphi.a^3}{t_c^3}+\frac{(cos^2\varphi).t_c}{a}\right]}\right)} \tag{3}$$

After deduction Eq. (4) can be obtained:

$$K = \frac{2.t_c}{a.\cos^2\varphi}.\left(\frac{\sin^2\varphi.a^3}{t_c^3} + \frac{\cos^2\varphi.t_c}{a}\right) \tag{4}$$

After rearranging Eq. (5) is obtained

$$K = 2.\left(\tan^2\varphi.\frac{a^2}{t^2} + \frac{t^2}{a^2}\right) \tag{5}$$

For the common honeycomb geometries, the ratio $\frac{t^2}{a^2}$ is very small and can be neglected. With the data from Table 1, a value of $\frac{t^2}{a^2}$ =1.08E-4 is reached. The K-factor can thus be reduced to Eq.(6).

$$K = \frac{2.a^2}{t^2} tan^2\varphi. \tag{6}$$

3. Determination of Orthotrope Parameter Values for Equivalent Layer

3.1. Definition of Honeycomb Sandwich

The honeycomb structure can be modified based on a set of defined parameters. The modification of these parameters leads to a change in structural properties of the honeycomb sandwich. The most common cell shape within a honeycomb sandwich is the one consisting of uniform hexagonal prism cells. As this cell shape is used most frequently, this one will be examined although more complex geometrical shapes exist. Figure 1 defines the parameters of the honeycomb cell geometry.

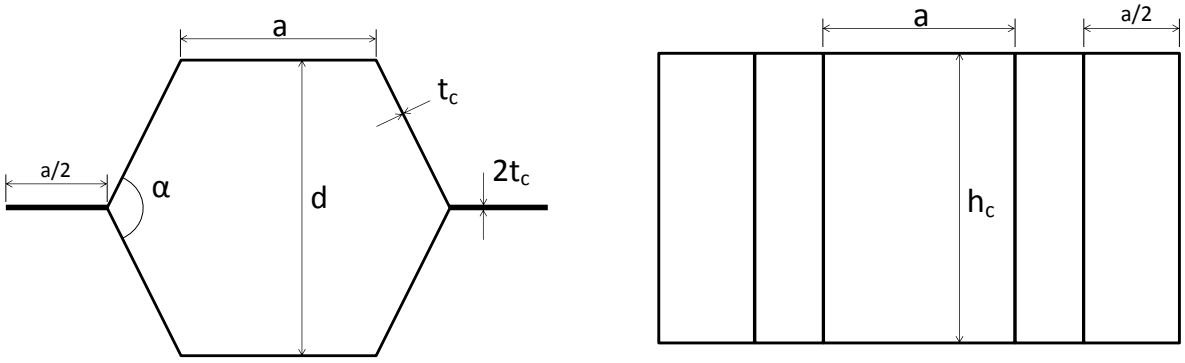

(a) Top view of cell

(b) Front view of cell

Figure 1: Honeycomb geometrical cell parameters

The main objective is to model the sandwich core as a orthotropic material layer. Resulting from literature study in Section 1.2 there are different studies carried out to determine these orthotropic parameter values. In order to determine a set of parameter values that can be used to model an equivalent sandwich layer in order to bypass time-consuming FE calculations, it is necessary to compare different approximative models. but also benchmark them against a detailed finite element model. As not all studies list formulas for the complete set of parameters, some studies will be combined in order to achieve a complete set of parameters. The parameters needed for this calculation, are listed in Table 1.

3.2. Finite Element Modeling

research is conducted on the design and analysis of equivalent core models, substituting the honeycomb core in sandwich structures, in the finite element program Siemens NX 8.0.

Table 1: Honeycomb parameters for the definition of the equivalent orthotropic material layer

Item	Property	Value
Cell dimensions	$t_c(mm)$	0,0381
	a(mm)	3,666
	$\alpha(^\circ)$	120
General dimensions	l(mm)	500
	b(mm)	102,6
	h(mm)	12,7
Elastic parameters	$E_w(N/mm^2)$	69 E+03
	$\nu_w()$	0.33
	$G_w(N/mm^2)$	26 E+03

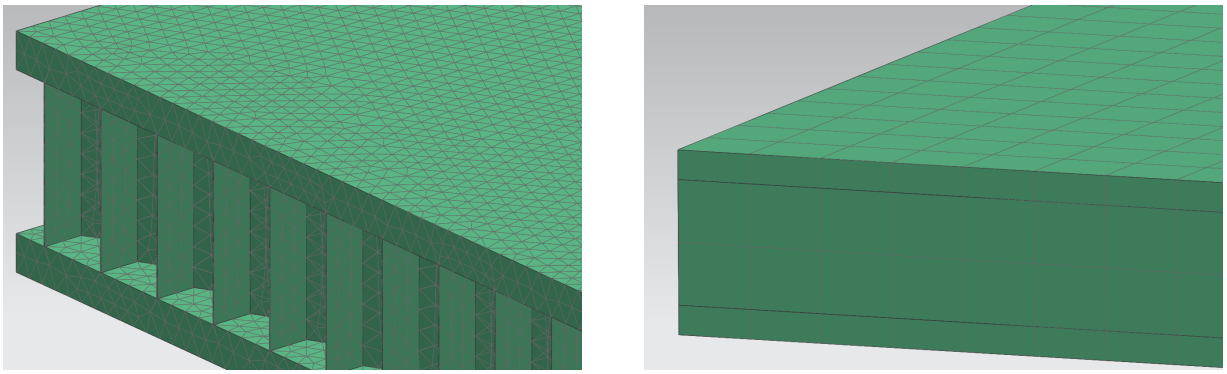

(a) complex FE model (b) equivalent FE model

Figure 2: higly detailed FE model versus equivalent model

Table 2: Comparison of complex reference model with equivalent model

Item	Reference Model 'CoHC'	Equivalent Model 'EqO1'
Element type	Tetra4	Hex8
Number of elements	840896	3276
Number of nodes	1443907	4480
Calculation time [s]	47440	2
Memory usage [MB]	4668	100
File size [MB]	1610	39

4. Calculation of Equivalent Sandwich Structure

4.1. Introduction

In order to minimize the calculation time of complex FE models, the complex geometry of the honeycomb model is replaced by an equivalent model. In order to achieve this, various models available from literature will be compared. These models will consist of a simple core

structure. Different material properties for the core structure will lead to different results and conclusions.

4.2. Orthotrope elastic properties

It is chosen to model the core material with orthotropic material properties. In this paper, it will be useful to combine different formulations in such a way that implementing these values in the finite element model yield meaningful output results with respect to the highly-detailed composite model. The candidate equivalent models with simplified geometry, as shown in Figure 2(b), are compared with the complex honeycomb model described in Figure 2(a).

It is necessary to compare the different approximations with each other. In Table 3, Table 4 and Table 5 the applied parameter values are listed. The geometric properties are listed in Table 1. One can notice that the approximative formula for E_1 by Abd El-Sayed [24] results in a value for $E_1 = 577.6N/mm^2$ while values resulting from Masters & Evans [22] en Nast [30] are a factor 3500 smaller. As demonstrated in Table 4 it is clear that the values for ν_{23} en ν_{13} are approaching zero for both applied models.

Table 3: Young's modulo orthotropic equivalent

Item	Model	Value
$E_1(N/mm^2)$	Masters & Evans [22]	0.179
	Nast [30]	0.163
	Abd El-Sayed [24]	577.556
$E_2(N/mm^2)$	Masters & Evans [22]	0.179
	Nast [30]	0.201
	Abd El-Sayed [24]	509.419
$E_3(N/mm^2)$	Nast [30]	1103.73
	Liu [23]	1103.73
	Zhang & Ashby [29]	1103.73

Table 4: Poisson's Ratios orthotropic equivalent

Item	Model	Value
ν_{12}	Masters & Evans [22]	1
	Nast [30]	0.752
	Abd El-Sayed [24]	1
ν_{23}	Nast [30]	6.00 E-05
	Zhang & Ashby [29]	0
ν_{13}	Nast [30]	7.81 E-05
	Zhang & Ashby [29]	0

Table 5: Shear modulus orthotropic equivalent

Item	Model	Value
$G_{12}(N/mm^2)$	Masters & Evans [22]	4.47 E-02
	Nast [30]	4.63 E-02
$G_{13}(N/mm^2)$	Grediac [25]	234.01
	Nast [30]	416.02
	Liu [23]	234.01
	Shi [26]	234.01
	Zhang & Ashby [29]	234.01
$G_{23}(N/mm^2)$	Grediac [25]	156.01
	Nast [30]	308.16
	Liu [23]	156.01
	Shi [26]	156.01
	Zhang & Ashby [29]	156.01

From Tables 3, 4 en 5, one can conclude that for the given parameter values, listed in Table 1 there is similarity to be detected in the approximations for the orthotropic elastic constants.

Next, the influence of the α-angle on the orthotropic elastic constants is examined. This angle mainly defines the hexagonal prism that defines the cell geometry, as shown in Figure 1.

In Fig. 3 the influence of the α-angle on the trend of the Young's moduli E_1 and E_2 values by Masters [22] and Nast [30] is demonstrated. From Figure 3 one can conclude that the values for the Young's modulus do not exceed $1N/mm^2$ for α between 65° and 150°. These values are much lower with respect to the calculated values for E_3. The approximations of Masters & Evans and Nast voor E_2 follow the same evolution but are diverging for E_1 at lower angle values. This difference is negligible compared to difference found with approximation [24]. From this figure, it is thus concluded that for the angle range of α between 105° and 150° the approximations for E_1 en E_2 can be used.

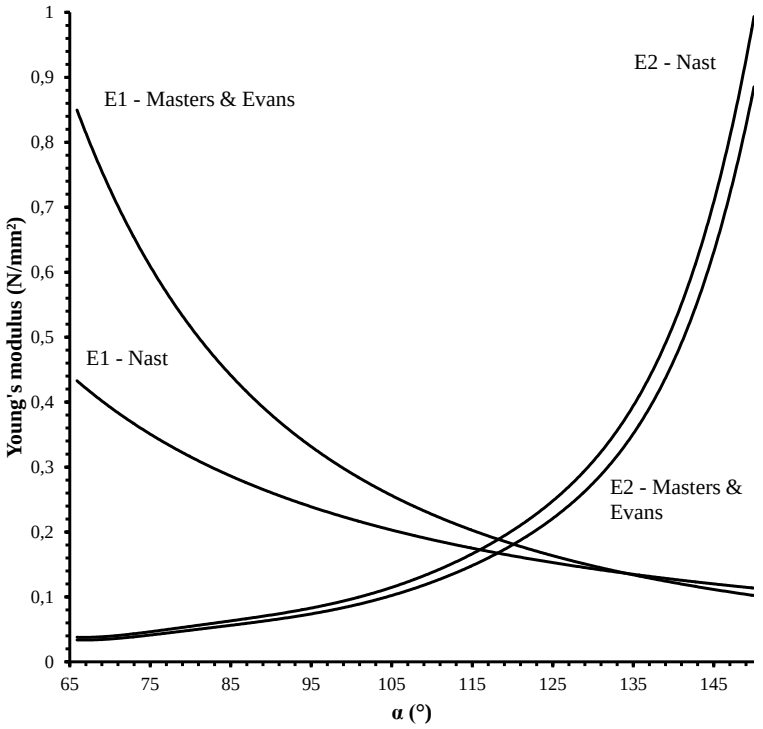

Figure 3: Influence of angle variation on Young's Modulus values.

5. Modeling the equivalent sandwich layer

A finite element (FE) model is generated that represents the equivalent structure with a sandwich layer. The model dimensions (length, width and height) are taken identical to the values of the complex FE model. The equivalent model consists of an equivalent core bounded by two sandwich outer plates. The mapped FE mesh is generated with brick elements. The model (Figure 4) consists of 3276 elements. A convergence test is carried out to check the mesh quality.

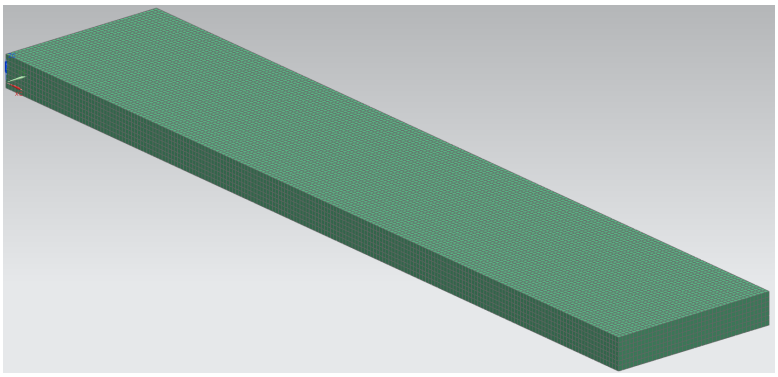

Figure 4: Equivalent honeycomb sandwich FE model.

In order to define and compare the various equivalent models, a code is defined for each model describing the type of model used during the finite element analysis. The used models and respective abbreviations are listed in Table 6 and Table 7.

Table 6: Denomination of different equivalent models

Item	Definition
CoHC	model with complex geometry
EqIso	equivalent model with solid isotropic core
EqOi	equivalent model with orthotropic core Oi

Approximative model EqO1 is based on the commonly used orthotropic parameters found in literature (Table 7). Model EqO2 is defined in order to examine alternative models and values for E_1 and E_2 with respect to approximative model EqO1. Other used models and values for G_{13} and G_{23} with respect to EqO1 are examined by the definition of model EqO3. The influence of v_{12} is examined in equivalent model EqO4. Table 7 gives an overview of the defined approximations for each of the nine elastic constants used in the four approximative equivalent models for the core composite layer.

Table 7: Definition orthotropic core

Property	Model O1	Model O2	Model O3	Model O4
E_1	Masters [22]	Abd El-Sayed [24]	Masters [22]	Masters [22]
E_2	Nast [30]	Abd El-Sayed [24]	Nast [30]	Masters [22]
E_3	Nast [30]	Liu [23]	Nast [30]	Liu [23]
v_{12}	Masters [22]	Masters [22]	Masters [22]	Nast [30]
v_{23}	Zhang [29]	Zhang [29]	Zhang [29]	Zhang [29]
v_{13}	Zhang [29]	Zhang [29]	Zhang [29]	Zhang [29]
G_{12}	Masters [22]	Masters [22]	Masters [22]	Masters [22]
G_{13}	Liu [23]	Liu [23]	Nast [30]	Grediac [25]
G_{23}	Grediac [25]	Grediac [25]	Nast [30]	Liu [23]

6. Discussion of Results

6.1. Loading Conditions

In this section the different analysis results will be compared and discussed. The equivalent models are subjected to a number of loading cases, listed in Table 8. Also the modal analysis results are used to compare the different models. The performance of the different approximations is compared with the highly detailed finite element model results.

These loading conditions are given a specific name depending on the direction of the applied load. For example, a clamped sandwich structure in the B-H plane and subject to an applied load in the L-direction, is defined as 'B,H,L' (Figure 5). This leads to a large number of possible

Table 8: Applied set of five loading conditions.

Item	Constraining	Direction $\vec{F}$	F(N)
B,H,H	B,H-face	H	250
B,L,L	B,L-face	L	250
B,L,H	B,L-face	H	250
B,L,B	B,L-face	B	250
H,L,H	L,H-face	H	250

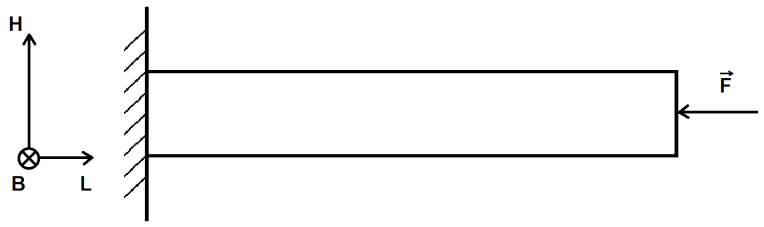

Figure 5: Definition of loading condition 'B,H,L'.

loading cases of which five were selected for comparison, as shown in Table 8. Not all loading cases are equally important because in some cases the honeycomb layer has little or no effect on the bending stiffness of the composite structure [31]. As a consequence, the remaining load cases to be used are listed in Table 8. In addition to the applied loading conditions, listed in Table 8, also a modal analysis is applied in order to compare the different equivalent models. The first four eigenfrequencies are analyzed and compared.

6.2. Static Deflections and Eigenfrequencies

The results for the 5 load cases are listed in Tables 9 and 10. Table 11 lists the results from the modal analysis.

Table 9: Calculated deflections for five applied load cases

Load Case	CoHc [mm]	EqO1 [mm]	Δ_1 [%]	EqO2 [mm]	Δ_2 [%]	EqO3 [mm]	Δ_3 [%]	EqO4 [mm]	Δ_4 [%]
BHH	4.1	4.26	3.90	4.2	2.44	4.14	0.98	4.26	3.90
BLL	2.55E-04	2.71E-04	6.27	7.74E-04	203.53	1.52E-04	40.39	2.79E-04	9.41
BLH	5.45E-05	5.88E-05	7.89	5.89E-05	8.07	5.90E-05	8.26	5.88E-05	7.89
BLB	4.20E-04	4.31E-04	2.62	4.38E-04	4.29	2.27E-04	45.95	4.20E-04	0.00
HLH	2.11E-02	2.04E-02	3.32	2.04E-02	3.32	1.36E-02	35.55	2.04E-02	3.32
Mean [%]			4.80		44.33		26.22		4.90

Table 10: Calculated deflections for 5 applied load cases in mm (cont'd)

Load Case	CoHc [mm]	EqIso [mm]	Δ_{iso} [%]
BHH	4.1	4.22	2.93
BLL	2.55E-04	1.54E-04	39.61
BLH	5.45E-05	4.00E-05	26.61
BLB	4.20E-04	1.66E-04	60.48
HLH	2.11E-02	1.17E-02	44.55
Mean [%]			34.83

From Table 9 one can conclude that the approximative model that yields overall the most accurate results with respect to the deflection values, is model 'EqO1' (mean difference of 4.8%), closely followed by model 'EqO4' (4.9% mean difference). The main difference is situated in loading condition BLL where model 'EqO4' is less accurate with a relative error of 9.4%. The least accurate approximative model with respect to deflection values, is model 'EqO2' yielding a mean difference of 44.3%. This is mainly due to the noticeable difference for loading condition BLL. When not taking into account this loading condition, model 'EqO2' yields a mean relative difference of 4.5% which has the same order of magnitude as model 'EqO1' (4.4%) and model 'EqO4' (3.8%). When looking at the deflection magnitude for the isotropic model 'EqIso' one can conclude that this model is the least accurate model with the highest relative difference for loading conditions BLH, BLB and HLH. One can thus conclude that this model is not acceptable as an approximative FE model for honeycomb composites.

Table 11: Calculated eigenfrequencies for five applied load cases

CoHc [Hz]	EqIso [Hz]	Δ [%]	EqO1 [Hz]	Δ [%]	EqO2 [Hz]	Δ [%]	EqO3 [Hz]	Δ [%]	EqO4 [Hz]	Δ [%]
496.30	518.9	4.55	493.10	0.64	495.4	0.18	517.4	4.25	493.1	0.64
843.20	994	17.90	834.70	1.01	835	0.98	991	17.58	835	1.01
1095.00	1220	11.60	1080.00	1.37	1080	1.19	1220	11.42	1080	1.37
1619.00	1840	13.47	1609.00	0.62	1610	0.56	1810	11.55	1610	0.62
Mean [%]		11.88		0.91		0.73		11.20		0.91

From Table 11 one can conclude that the approximative model that yields the most accurate overall results with respect to the eigenfrequencies values, is model 'EqO2' (mean difference of 0.7%), closely followed by model 'EqO4' (0.9% mean difference) but also model 'EqO1' (0.9% mean difference). Model 'EqO2' scores best on all 4 eigenfrequencies and the difference with respect to 'EqO1' and 'EqO4' is mainly due to eigenfrequency 1 which is the frequency of the first bending mode. The least accurate model is again model 'EqIso' with a mean difference of 11.9%. One can thus conclude that an isotropic equivalent model is does not yield accurate results and is not to be chosen as equivalent model to replace the honeycomb layer. Thus it is necessary to use an equivalent orthotropic material layer.

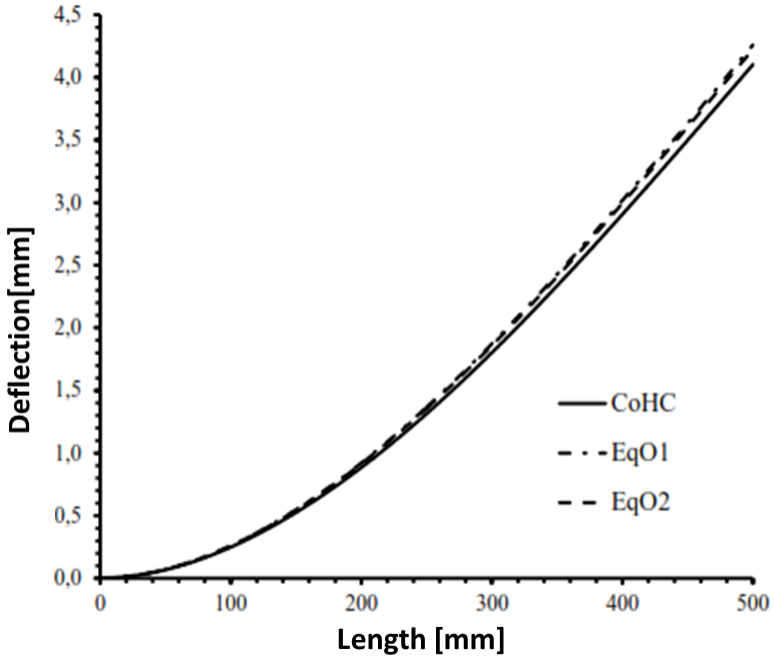

Figure 6: Deflections of models CoHC, EqO1 and EqO2 for load case BHH.

When looking for an overall most suitable accurate model, one can notice that 'EqO1' and model 'EqO4' only slightly differ with respect to average relative differences. The reason that model 'EqO2' does not score on the same level as 'EqO4', is only due to the difference with respect to deflection from loading condition BLL. From these results it is clear that model 'EqO3' shows important differences for loading cases BLL, BLB en HLH. Once can thus conclude that the approximative model developed by E. Nast [30] for G_{13} en G_{23} insufficiently approximates the complex model.

Despite the fact that the approximations for E_1 and E_2 show strong differences between each other (model 'EqO1' and 'EqO2' only differentiate in the approximation for E_1 and E_2), there is no significant difference, nor on the level of eigenfrequencies neither on the level of displacement amplitudes. One can conclude from the results that models 'EqO1' and 'EqO2' yield very close results with respect to each other. Figure 6 visualizes the three fine models in 400 nodes along the principal direction of the sandwich beam. It is clear that the two equivalent models approximate the fine honeycomb model accurately. Once can conclude from the simulation results that the deflections values but also eigenfrequencies do not deviate more than 4% with 'EqO1' and 'EqO2'.

6.3. Stress Analysis of an Equivalent Material Layer

In Figure 7 the stress distribution of load case BHH is displayed. One can notice that the outer layers reach a maximum stress value of $22MPa$. This stress magnitude is also present in the equivalent models, as visualized in Figure 8 for model 'EqO1'. Based on this result,one can conclude that the equivalent models yield stress values that closely match these of the highly-detailed model.

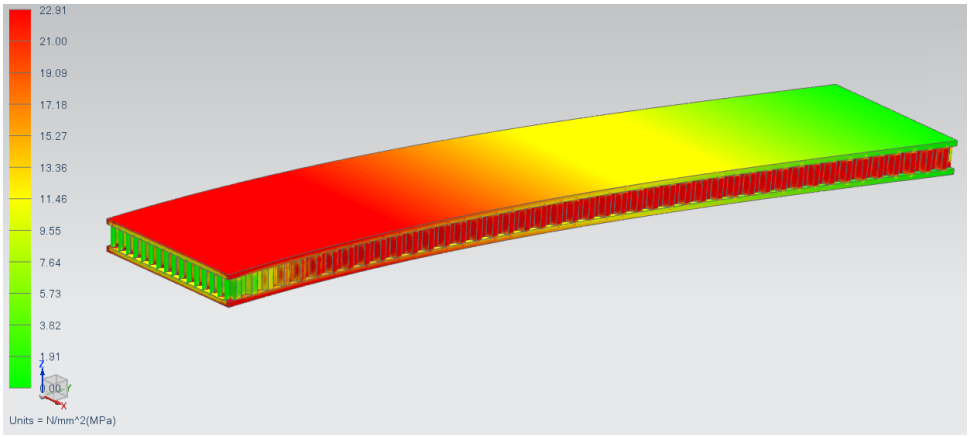

Figure 7: Stress outline model 'CoHc' with BHH loading.

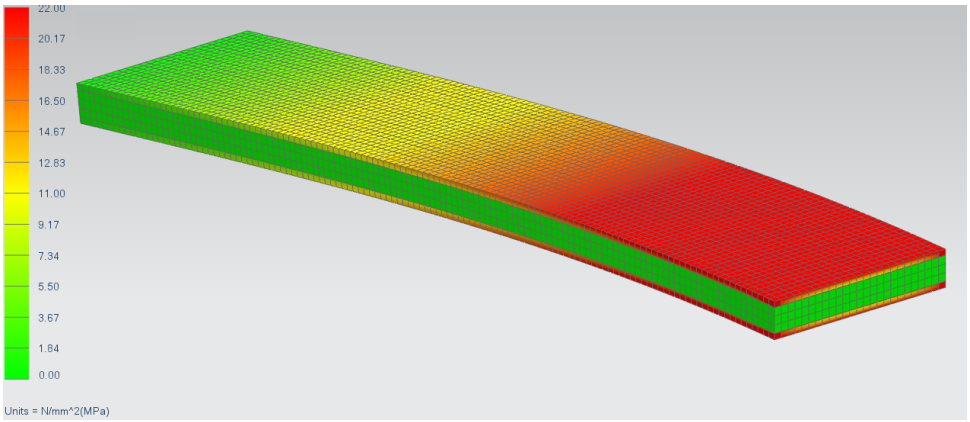

Figure 8: Stress outline equivalent model 'EqO1' with BHH loading.

The largest benefit of using the equivalent model is shown in Table 2, where the complexity and computational effort (time and storage) of the two models are compared. The values are listed for the modal analysis calculations presented in Table 11. When comparing these results, one can notice that the calculation time is reduced with an order of magnitude 10^5. This is also noticeable in the necessary file size of the saved calculation results. A reduction of the number of nodes with a factor 322 is also achieved. It is noteworthy that even a model with 12 honeycomb cells needs a considerable calculate time of 13 hours. In reality, honeycomb sandwich models with more than 10000 cells are common, resulting in even higher computation times. By making use of equivalent models containing optimized orthotropic material parameter values resulting from approximate formulas, these high computation times can be eliminated without straying too far from the exact solutions.

7. Conclusion

From running simulations, it is easy to state that finite element models containing honeycomb sandwich layers are yielding high computation times. The main goal of this research

paper is to define an appropriate equivalent model in order to minimize the complexity of the finite element model and thus minimize FE calculation time. In order to minimize these computation times, but also the time to create a highly detailed honeycomb sandwich layer, an equivalent model with the right set of material property values is defined based on literature study on the available models. The most accurate equivalent model consists of one continuous layer with orthotropic elastic constants and calculated values based on different available approximate formulas. This way the complex geometry does not need to be created while the model yields sufficiently accurate results.

When comparing these results, one can notice that the calculation time is reduced with order of magnitude 10^5. This is also noticeable in the necessary file size of the saved calculation results. A reduction of the number of nodes with a factor 322 is also achieved. This is the most important results of this research, in order to minimize FE calculation times as the complex FE honeycomb models needs 13h to calculate the output results. It is noteworthy that even a model with 12 honeycomb cells needs this huge calculate time. In reality, honeycomb sandwich models with more than 10000 cells are common, resulting in even higher computation times. By making use of equivalent models containing optimized orthotropic material parameter values resulting from approximate formulas, these high computation times can be eliminated.

Acknowledgements

This research has been funded by the University of Antwerp and the Institute for the Promotion of Innovation by Science and Technology in Flanders (IWT) by the support to the TETRA project 'Smart data clouds' with project number 140336. Furthermore, the research leading to these results has received funding from Industrial Research Fund FWO Krediet aan navorsers 1.5.240.13N. The authors also acknowledge the Flemish government (GOA-Optimech) and the research councils of the Vrije Universiteit Brussel (OZR) and University of Antwerp (fti-OZC) for their funding.

Nomenclature list

Dimensions sandwich structure

Parameter	Unit	Description
t_c	mm	thickness of honeycomb cell following Figure 1
h_c	mm	height of honeycomb cell following Figure 1
a	mm	length of hexagon side following Figure 1
d	mm	size of honeycomb cell following Figure 1
α	rad	characteristic large angle of the hexagonal prism following Figure 1
φ	rad	characteristic small angle of the hexagonal prism
t	mm	thickness of sandwich
L_t	mm	length of unity cell
B_t	mm	width of unity cell
B	/	width direction of sandwich structure
H	/	height direction of sandwich structure
L	/	length direction of sandwich structure
b	mm	width of the sandwich structure
h	mm	total height of the sandwich structure
l	mm	length of the sandwich structure
K		calculation parameter of the simplified formulas

Elasticity parameters

Parameter	Unit	Description
E_w	MPa	Young's modulus of the sandwich wall
E_k	MPa	Young's modulus of the core material
G_w	MPa	Shear modulus of the sandwich wall
G_k	MPa	Shear modulus of the core material
ν_w	/	Poisson's ratio sandwich wall
ν_k	/	Poisson's ratio core material
E_i	MPa	Young's modulus orthotropic equivalent in the i direction
G_{ij}	MPa	Shear modulus orthotropic equivalent in the j direction on the normal face of direction i
ν_{ij}	/	Poisson's ratio orthotropic equivalent. Contraction in the j direction by extension in the i direction
C_{ij}	/	Calculation parameter Hooke's law
Δ	/	Calculation parameter Hooke's law
D	Nmm^2	Bending stiffness (equal to E.I)
ρ_k	g/cm^3	density of the solid core
ρ_w	g/cm^3	density of the sandwich walls

Addendum: Orthotropic elastic constants

All in literature described different approaches of the determination of the nine orthotropic elastic constants are tabulated in this addendum. The definition of the used coordinate system reference is shown in Figure 9. The explanation of the used symbols is found in the nomenclature list.

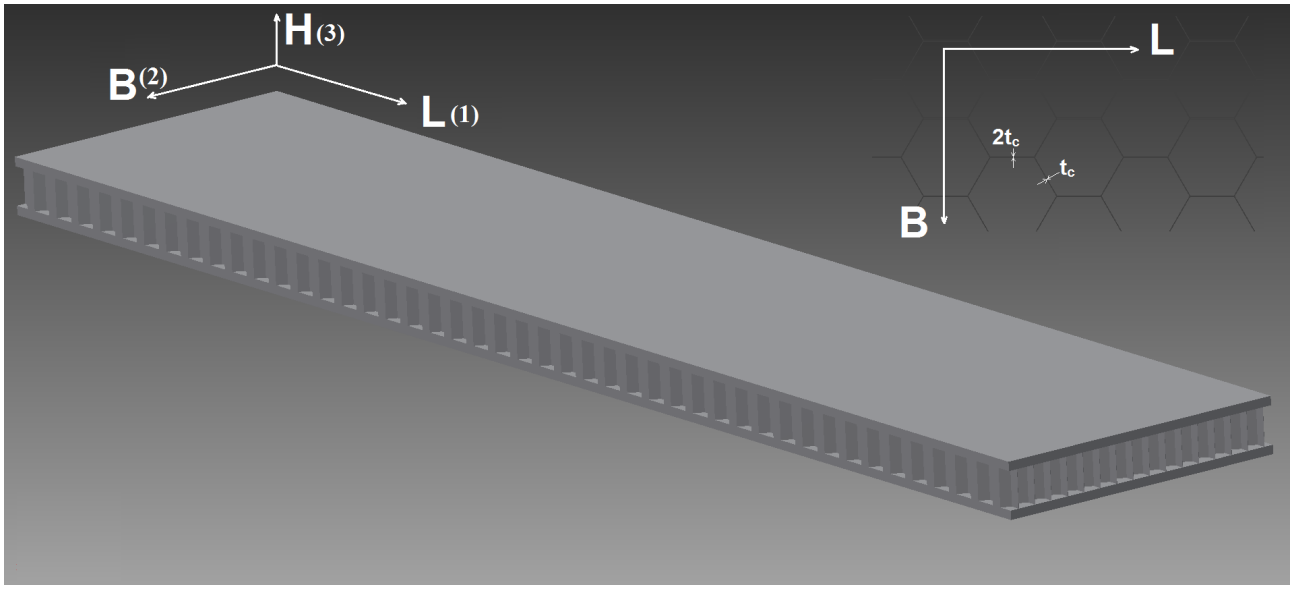

Figure 9: Reference system

Calculation E_1

Masters & Evans [22]

$$E_1 = \frac{E}{\frac{\cos\varphi}{1+\sin\varphi}.\left[\frac{\cos^2\varphi.a^3}{t_c^3} + \frac{(2+\sin^2\varphi).t_c}{a}\right]} \tag{7}$$

Nast [30]

$$E_1 = \frac{t_c^3.(1+\sin\varphi).E}{12a^3.\cos^2\varphi.\left[\frac{1-\cos\varphi}{8} + \frac{\cos\varphi}{12}\right].(1-\nu^2)} \tag{8}$$

Abd El-Sayed [24]

$$E_1 = \frac{6.cos\varphi.\tan^2\varphi.t_c.E}{\left[\frac{a^2}{4.\tan^2\varphi.h_c^2} + \sin\varphi + a.\frac{\cos\varphi}{2}\right].a} \tag{9}$$

Calculation E_2

Masters & Evans [22]

$$E_2 = \frac{E}{\frac{1+\sin\varphi}{\cos\varphi}.\left[\frac{\sin^2\varphi.a^3}{t_c^3} + \frac{(cos^2\varphi).t_c}{a}\right]} \tag{10}$$

Nast [30]

$$E_2 = \frac{E.t_c^3.\cos\varphi}{(1+\sin\varphi).a^3.\sin^2\varphi.(1-\nu^2)} \tag{11}$$

Abd El-Sayed [24]

$$E_2 = \frac{2.E.t_c.\cos\varphi}{3.\left[\frac{a^2}{4.\tan^2\varphi.h_c^2} + \cos^2\varphi\right].a} \tag{12}$$

Calculation E_3

Universally accepted(Nast, Liu, Zhang)[30, 23, 29]

$$E_3 = \frac{2.E.t_c}{\cos\varphi.(1+\sin\varphi).a} \tag{13}$$

Calculation G_{12}

Masters & Evans [22]

$$G_{12} = \frac{E}{\frac{3.\cos\varphi.a^3}{(1+\sin\varphi).t_c^3} + \left[\cos\varphi + a.\tan\varphi.(1+\sin\varphi)\right].\frac{a}{t_c}} \tag{14}$$

Nast [30]

$$G_{12} = \frac{E.t_c^3.(\sin\varphi+1)}{a^3.(1-\nu^2).\cos\varphi.(6,25-6.\sin\varphi)} \tag{15}$$

Calculation G_{23}

Liu, Grediac, Zhang [23, 25, 29]

$$G_{23} = \frac{\cos\varphi.t_c.G}{(1+\sin\varphi).a} \tag{16}$$

Nast [30]

$$G_{23} = \frac{10.t_c.G}{9.(1+\sin\varphi).a.\cos\varphi^3} \tag{17}$$

Shi [26]

$$G_{23} = \frac{\tan\varphi.t_c.G}{a} \tag{18}$$

Calculation G_{13}

Liu [23]

$$G_{13} = \frac{(1+\sin\varphi).G.t_c}{2.\cos\varphi.a} \tag{19}$$

Nast [30]

$$G_{13} = \frac{2.G.t_c}{\cos\varphi.a(1+\sin\varphi)} \tag{20}$$

Shi [26]

$$G_{13} = \frac{3.G.t_c.\tan\varphi}{2.a} \tag{21}$$

Grediac, Ashby [25, 29]

$$G_{13} < \frac{(1+\sin^2\varphi).G.t_c}{(1+\sin\varphi).\cos\varphi.a} \tag{22}$$

$$G_{13} > \frac{(1+\sin\varphi).G.t_c}{2.\cos\varphi.a} \tag{23}$$

Calculation ν_{12}

Masters & Evans [22]

$$\nu_{12} = \frac{(1+\sin\varphi).\sin\varphi}{\cos^2\varphi} \tag{24}$$

Nast [30]

$$\nu_{12} = \frac{(1+\sin\varphi).\sin^2\varphi}{12.\cos^2\varphi.\left[\frac{\cos\varphi}{3} - \frac{1+\cos\varphi}{8}\right]} \tag{25}$$

Abd El-Sayed [24]

$$\nu_{12} = 3.\tan^2\varphi \tag{26}$$

Calculation ν_{23}

Nast [30]

$$\nu_{23} = \frac{t_c^2.\cos^2\varphi.\nu}{2.a^2.\sin^2\varphi.(1-\nu^2)} \tag{27}$$

Calculation ν_{13}

Nast [30]

$$\nu_{13} = \frac{t_c^2.(1+\sin\varphi)^2.\nu}{24.a^2.\cos\varphi.\left[\frac{\cos\varphi}{3} - \frac{1+\cos\varphi}{8}\right].(1-\nu^2)} \tag{28}$$

References

[1] J. Kee Paik, A. K. Thayamballi, G. Sung Kim, The strength characteristics of aluminum honeycomb sandwich panels, ThinWalled Structures 35 (3) (1999) 205–231. doi:10.1016/S0263-8231(99)00026-9.
URL http://linkinghub.elsevier.com/retrieve/pii/S0263823199000269

[2] A. Abbadi, Y. Koutsawa, A. Carmasol, S. Belouettar, Z. Azari, Experimental and numerical characterization of honeycomb sandwich composite panels, Simulation Modelling Practice and Theory 17 (10) (2009) 1533–1547. doi:10.1016/j.simpat.2009.05.008.
URL http://linkinghub.elsevier.com/retrieve/pii/S1569190X09000604

[3] S. D. Papka, S. Kyriakides, Experiments and full-scale numerical simulations of in-plane crushing of a honeycomb, Acta Materialia 46 (8) (1998) 2765–2776. doi:10.1016/S1359-6454(97)00453-9.
URL http://linkinghub.elsevier.com/retrieve/pii/S1359645497004539

[4] X. E. Guo, L. J. Gibson, Behavior of Intact and Damaged Honeycombs: a Finite Element Study, International Journal of Mechanical Sciences 41 (1) (1999) 85–105.

[5] D. Ruan, G. Lu, B. Wang, T. X. Yu, In-plane dynamic crushing of honeycombsa finite element study, International Journal of Impact Engineering 28 (2) (2002) 161–182. doi:10.1016/S0734-743X(02)00056-8.
URL http://linkinghub.elsevier.com/retrieve/pii/S0734743X02000568

[6] Z. Zou, Reid, P. Tan, S. Li, J. Harrigan, Dynamic crushing of honeycombs and features of shock fronts, International Journal of Impact Engineering 36 (1) (2009) 165–176.
URL http://discovery.ucl.ac.uk/170690/

[7] Z. Zheng, J. Yu, J. Li, Dynamic crushing of 2D cellular structures: A finite element study, International Journal of Impact Engineering 32 (1-4) (2005) 650–664. doi:10.1016/j.ijimpeng.2005.05.007.
URL http://linkinghub.elsevier.com/retrieve/pii/S0734743X05000795

[8] C. C. Chamis, R. A. Aiello, P. L. N. Murthy, Apparent properties of a honeycomb core sandwich panel by numerical experiments, Journal of Composites Technology and Research 10 (1988) 93–99.

[9] U. Karlsson, N. Wetteskog, Ekvivalenta Styvhetsparametrar för Honeycomb, Master's thesis, Chalmers Tekisnka Högskola, Zweden (1987).

[10] R. M. Martinez, Apparent properties of a honeycomb core sandwich panel by numerical experiment, Master's thesis, University of Texas (1989).

[11] W. Elspass, Thermostabile Strukturen in Sandwichbauweise, Ph. d. thesis, Eidgenössische Technische Hochschule Zürich, Switzerland (1989).

[12] W. Elspass, Design of High Precision Sandwich Structures Using Analytical and Finite Element Models, in: 6th World Congress on Finite Element Methods, Banff, Canada, 1990, pp. 658–664.

[13] S. Mistou, M. Sabarots, M. Karama, Experimental and numerical simulations of the static and dynamic behaviour of sandwich plates, in: European Congress on Computational Methods in Applied Sciences and Engineering, Barcelona, Spanje, 2000.

[14] C. C. Foo, G. B. Chai, L. K. Seah, A model to predict low-velocity impact response and damage in sandwich composites, Composites Science and Technology 68 (6) (2008) 1348–1356. doi:10.1016/j.compscitech.2007.12.007.
URL http://www.sciencedirect.com/science/article/pii/S0266353807004757

[15] G. Allegri, U. Lecci, M. Machetti, F. Poscente, FEM Simulation of the Mechanical Behaviour of Sandwich Materials for Aerospace Structures, Key Engineering Materials 221-222 (2002) 209–220.

[16] L. Gornet, S. Marguet, G. Marckmann, Failure and Effective Elastic Properties Predictions of Nomex Honeycomb Cores, in: 12th European Conference on Composite Materials, Biarritz, Frankrijk, 2006.

[17] J. Hohe, W. Becker, Effective stress-strain relations for two-dimensional cellular sandwich cores: Homogenization, material models, and properties, Applied Mechanics Reviews 55 (1) (2002) 61. doi:10.1115/1.1425394.
URL http://link.aip.org/link/AMREAD/v55/i1/p61/s1&Agg=doi

[18] K. Li, X. L. Gao, J. Wang, Dynamic crushing behavior of honeycomb structures with irregular cell shapes and non-uniform cell wall thickness, International Journal of Solids and Structures 44 (14-15) (2007) 5003–5026. doi:10.1016/j.ijsolstr.2006.12.017.
URL http://linkinghub.elsevier.com/retrieve/pii/S0020768306005427

[19] M.-Y. Yang, J.-S. Huang, J. W. Hu, Elastic Buckling of Hexagonal Honeycombs with Dual Imperfections, Composite Structures 82 (3) (2008) 326–335.

[20] A. E. Simone, L. J. Gibson, Effects of solid distribution on the stiffness and strength of metallic foams, Acta Materialia 46 (6) (1998) 2139. doi:10.1016/S1359-6454(97)00421-7.
URL http://linkinghub.elsevier.com/retrieve/pii/S1359645497004217

[21] A. E. Simone, L. J. Gibson, The effects of cell face curvature and corrugations on the stiffness and strength of metallic foams, Acta Materialia 46 (11) (1998) 3929–3935. doi:10.1016/S1359-6454(98)00072-X.
URL http://linkinghub.elsevier.com/retrieve/pii/S135964549800072X

[22] I. G. Masters, K. E. Evans, Models for the elastic deformation of honeycombs, Composite Structures 35 (4) (1996) 403–422. doi:10.1016/S0263-8223(96)00054-2.
URL http://linkinghub.elsevier.com/retrieve/pii/S0263822396000542

[23] Q. Liu, Y. Zhao, Effect of Soft Honeycomb Core on Flexural Vibration of Sandwich Panel using Low Order and High Order Shear Deformation Models, Journal of Sandwich Structures and Materials 9 (2007) 95–108.

[24] F. K. A. El-Sayed, R. Jones, I. W. Burgess, A theoretical approach to the deformation of honeycomb based composite materials, Composites 10 (4) (1979) 209–214. doi:10.1016/0010-4361(79)90021-1.
URL http://www.sciencedirect.com/science/article/pii/0010436179900211

[25] M. Grediac, A finite element study of the transverse shear in honeycomb cores, International Journal of Solids and Structures 30 (13) (1993) 1777–1788. doi:10.1016/0020-7683(93)90233-W.
URL http://linkinghub.elsevier.com/retrieve/pii/002076839390233W

[26] G. Shi, P. Tong, Equivalent transverse shear stiffness of honeycomb cores, International Journal of Solids and Structures 32 (10) (1995) 1383–1393. doi:10.1016/0020-7683(94)00202-8.
URL http://linkinghub.elsevier.com/retrieve/pii/0020768394002028

[27] S. Kelsey, R. A. Gellatly, B. W. Clark, The Shear Modulus of Foil Honeycomb Cores: A Theoretical and Experimental Investigation on Cores Used in Sandwich Construction, Aircraft Engineering and Aerospace Technology 30 (10) (1958) 294–302.

doi:10.1108/eb033026.
URL http://www.emeraldinsight.com/10.1108/eb033026

[28] W. Becker, Closed-form analysis of the thickness effect of regular honeycomb core material, Composite Structures 48 (1-3) (2000) 67–70. doi:10.1016/S0263-8223(99)00074-4.
URL http://linkinghub.elsevier.com/retrieve/pii/S0263822399000744

[29] J. Zhang, M. F. Ashby, The out-of-plane properties of honeycombs, International Journal of Mechanical Sciences 34 (6) (1992) 475–489. doi:10.1016/0020-7403(92)90013-7.
URL http://linkinghub.elsevier.com/retrieve/pii/0020740392900137

[30] E. Nast, On honeycomb-type core moduli, in: 38th Structures, Structural Dynamics, and Materials Conference, Structures, Structural Dynamics, and Materials and Co-located Conferences, American Institute of Aeronautics and Astronautics, 1997. doi:doi:10.2514/6.1997-1178.
URL http://dx.doi.org/10.2514/6.1997-1178

[31] T. Legon, The equivalent modeling and analysis of aluminum honeycomb structures, a finite element study, Master's thesis, Artesis University College (2013).